Electronic Supplementary Material (ESI) for Catalysis Science & Technology.

SUPPLEMENTARY INFORMATION

MOF/TiO_2 erythrocyte-like heterostructures decorated by noble metals for use in hydrogen photogeneration and pollutant photodegradation

Mateusz A. Baluk[1], Paweł Mazierski[1], Aleksandra Pieczyńska[1], Kostiantyn Nikiforow[2], Grzegorz Trykowski[3], Tomasz Klimczuk[4], Adriana Zaleska-Medynska[1*]*

[1]Department of Environmental Technology, Faculty of Chemistry, University of Gdansk, Wita Stwosza 63, 80-308 Gdansk, Poland

[2]Institute of Physical Chemistry, Polish Academy of Science, Kasprzaka 44/52, 01-224 Warsaw, Poland

[3]Faculty of Chemistry, Nicolaus Copernicus University, Torun 87-100, Poland

[4]Department of Solid State Physics, Faculty of Applied Physics and Mathematics, Gdansk University of Technology, 80-233 Gdansk, Poland

*Adriana Zaleska-Medynska: adriana.zaleska-medynska@ug.edu.pl

*Mateusz A. Baluk: mateusz.baluk@phdstud.ug.edu.pl

P

Table S1. Particle size analysis of MOFs, h-MOFs, and ch-MOFs and the resulting noble metal nanoparticles (average of 100 counts).

Sample	Size of particles (nm)	Size of noble metal nanoparticles (nm)
MOFs	width: 738.4 ± 235.9 thickness: 160.3 ± 24.4	-
MOFs/Au		47.0 ± 6.5
h-MOFs	width: 998.6 ± 241.6 thickness: 187.2 ± 42.7	-
h-MOFs/Au		98.3 ± 54.6
h-MOFs/Au0.5%		85.3 ± 37.3
h-MOFs/Au2.0%		108.8 ± 32.6
h-MOFs/Ag		38.7 ± 8.3
h-MOFs/Pt		26.6 ± 7.1
h-MOFs/Pd		113 ± 51.1
h-MOFs (total)	irregular	-
ch-MOFs	width: 393.2 ± 115.5 thickness: 94.5 ± 17.9	-
ch-MOFs/Au		33.8 ± 12.1
ch-MOFs/Ag		29.9 ± 7.7
ch-MOFs/Pt		41.9 ± 12.2
ch-MOFs/Pd		34.6 ± 15.7

Table S2. Determination of the chemical composition of h-MOFs and h-MOFs/Au by TEM/EDX analysis.

Area (sample)	Weight composition (%)	Atomic composition (%)
Area 1 (h-MOFs)	C 62.36%, N 5.92% O 17.94%, Ti 13.76%	C 73.92%, N 6.01% O 15.96%, Ti 4.09%
Area 2 (h-MOFs)	C 62.53%, N 6.40% O 16.74%, Ti 13.31%	C 74.80%, N 6.46% O 14.80%, Ti 3.93%
Area 3 (h-MOFs)	C 59.07%, N 6.39% O 22.67%, Ti 11.85%	C 69.86%, N 6.48% O 20.13%, Ti 3.51%
Area 4 (h-MOFs)	C 55.71%, N 2.97% O 11.20%, Ti 30.07%	C 75.06%, N 3.44% O 11.33%, Ti 10.16%
Area 5 (h-MOFs/Au)	C 35.73%, N 1.71% O 5.19%, Ti 15.79% Au 41.56%	C 75.07%, N 3.08% O 8.19%, Ti 8.31% Au 5.32%

Table S3. Results of the XPS analysis of the MOF and h-MOF samples.

	MOFs		h-MOFs	
	Position, eV B.E.	Concentration, %At	Position eV B.E.	Concentration, %At
O 1s a (Ti-O)	530.22	**9.18**	530.54	**1.42**
O 1s b (C=O)	531.78	**19.29**	531.85	**15.29**
O 1s c (-OH)	532.61	**3.36**	533.59	**18.4**
		31.83		**35.11**
Ti 2p a	458.88	**6**	458.6	**1.45**
Ti 2p b	457.35	**0.36**	459.72	**0.9**
		6.36		**2.35**
N 1s a (-NH_2)	399.57	**5.09**	399.11	**0.11**
N 1s b (res. DMF)	401.05	**1.04**	401.03	**0.27**
N 1s c (-NH^+)	402.93	**1.21**	402.98	**1.31**
		7.34		**1.69**
C 1s a (C-C)	284.8	**28.25**	284.8	**19.25**
C 1s b (C-O)	286.2	**9.1**	286.15	**16.73**
C 1s c (C-N, C=O)	286.96	**5.93**	286.9	**14.41**
C 1s d (COOH)	288.76	**10.41**	288.88	**6.61**
C 1s e (Pi electrons)	290.7	**0.79**	291	**3.85**
		54.48		**60.85**

Table S4. Results of the XPS analysis of the ch-MOF sample.

	ch-MOFs	
	Position, eV B.E.	Concentration, %At
O 1s a (Ti-O)	529.98	**55.03**
O 1s b (Ti-O vac)	530.97	**5.64**
O 1s c (C=O)	532.01	**2.73**
		63.4
Ti 2p	458.73	**25.33**
		25.33
N 1s	400.4	**0.46**
		0.46
C 1s a (C-C)	284.8	**8.15**
C 1s b (C-O)	286.42	**1.19**
C 1s d (COOH)	289.06	**1.47**
		10.81

Table S5. Results of the XPS analysis of the h-MOF/M samples.

	h-MOF/Au		h-MOF/Ag		h-MOF/Pd		h-MOF/Pt	
	Position, eV BE	Concentration, %at	Position, eV BE	Concentration, %at	Position, eV BE	Concentration, %at	Position, eV BE	Concentration, %at
O 1s a (Me-O)	530.56	**1.12**	530.44	**0.91**	530.49	**1.05**	530.67	**1.78**
O 1s b (C=O)	531.93	**15.68**	531.89	**15.7**	531.9	**15.3**	531.89	**15.38**
O 1s c (C-O)	533.63	**18.64**	533.62	**18.48**	533.57	**18.02**	533.59	**17.77**
O		**35.44**		**35.09**		**34.37**		**34.93**
Ti 2p a (Ti_2O_3)	458.57	**1.35**	458.52	**1.29**	458.59	**1.44**	458.61	**1.42**
Ti 2p b (TiO_2)	459.85	**0.64**	459.82	**0.63**	459.96	**0.67**	459.74	**0.87**
Ti		**1.99**		**1.92**		**2.11**		**2.29**
N 1s a (C-N)			399.78	**0.1**				
N 1s b (res. DMF)	400.92	**0.33**	401.4	**0.15**	400.93	**0.37**	400.57	**0.2**
N 1s b ($-NH^+$)	402.99	**1.19**	403.03	**0.98**	402.93	**1.03**	402.87	**0.9**
N		**1.52**		**1.23**		**1.4**		**1.1**
C 1s a (C-C)	284.8	**21.1**	284.78	**20.26**	284.78	**22.29**	284.8	**22.25**
C 1s b (C-O)	286.17	**15.82**	286.13	**16.13**	286.21	**17.57**	286.23	**18.45**
C 1s c (C-N, C=O)	286.89	**14.3**	286.88	**13.65**	286.88	**12.14**	286.89	**9.27**
C 1s d (COOH)	288.9	**6.65**	288.84	**6.28**	288.88	**6.89**	288.85	**6.33**
C 1s e (pi electrons)	291.21	**3.13**	290.89	**5.09**	291.13	**3.22**	290.67	**3.97**
							293.45	**1.41**
C		**61**		**61.41**		**62.11**		**61.68**
Metal	85.1	**0.03**	369.01	**0.33**	338.19	**0.02**		**0**
		0.03		**0.33**		**0.02**		**0**
	Au 4f		Ag 3d		Pd 3d		Pt 4f	

Table S6. Results of the XPS analysis of the ch-MOF/M samples.

	ch-MOF/Au		ch-MOF/Ag		ch-MOF/Pd		ch-MOF/Pt	
	Position, eV BE	Concentration, %at	Position, eV BE	Concentration, %at	Position, eV BE	Concentration, %at	Position, eV BE	Concentration, %at
O 1s a (Me-O)	530.01	**55.62**	529.74	**44.58**	529.92	**48.58**	529.82	**50.8**
O 1s a (Me-O vacancy)			530.55	**6.25**	530.8	**4.99**	530.84	**6.17**
O 1s b (C=O)	531.31	**4.58**	531.64	**3.19**	531.82	**3.59**	531.89	**3.51**
O 1s c (C-O)	532.46	**2.41**	532.56	**1.16**	532.83	**0.95**		
O		**62.61**		**55.18**		**58.11**		**60.48**
Ti 2p (TiO_2)	458.74	**24.08**	458.51	**21.85**	458.68	**22.51**	458.57	**23.07**
Ti		**24.08**		**21.85**		**22.51**		**23.07**
N 1s a (C-N)	400.22	**1.27**	400.42	**1.08**	400.35	**0.91**	400.12	**0.82**
N		**1.27**		**1.08**		**0.91**		**0.82**
C 1s a (C-C)	284.83	**7.74**	284.8	**14.88**	284.84	**14.22**	284.8	**10.53**
C 1s b (C-O)	286.15	**2.81**	286.27	**3.63**	286.25	**2.4**	286.19	**3.29**
C 1s c (C-N, C=O)			288.41	**0.97**	288.04	**0.66**		
C 1s d (COOH)	288.99	**1.33**	289.27	**1.63**	289.11	**1.05**	288.67	**1.61**
C		**11.88**		**21.11**		**18.33**		**15.43**
Metal	83.29	**0.16**	367.36	**0.62**	340.24	**0.08**	70.26	**0.19**
			368.06	**0.17**	342.01	**0.06**	72.9	**0.02**
		0.16		**0.79**		**0.14**		**0.21**
	Au 4f		Ag 3d		Pd 3d		Pt 4f	

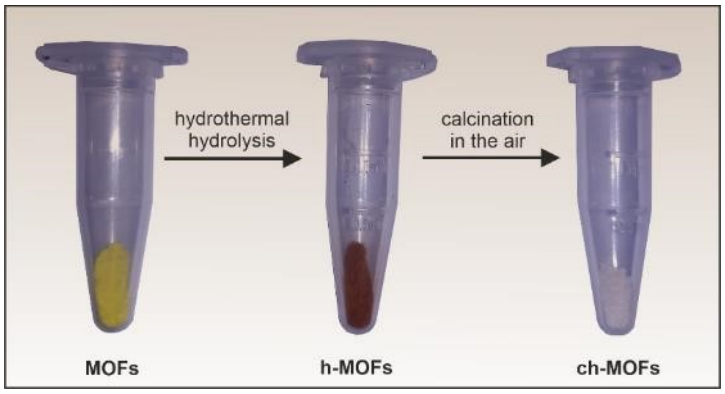

Fig. S1. Images of the samples obtained (from right to left: MOFs, h-MOFs, and ch-MOFs).

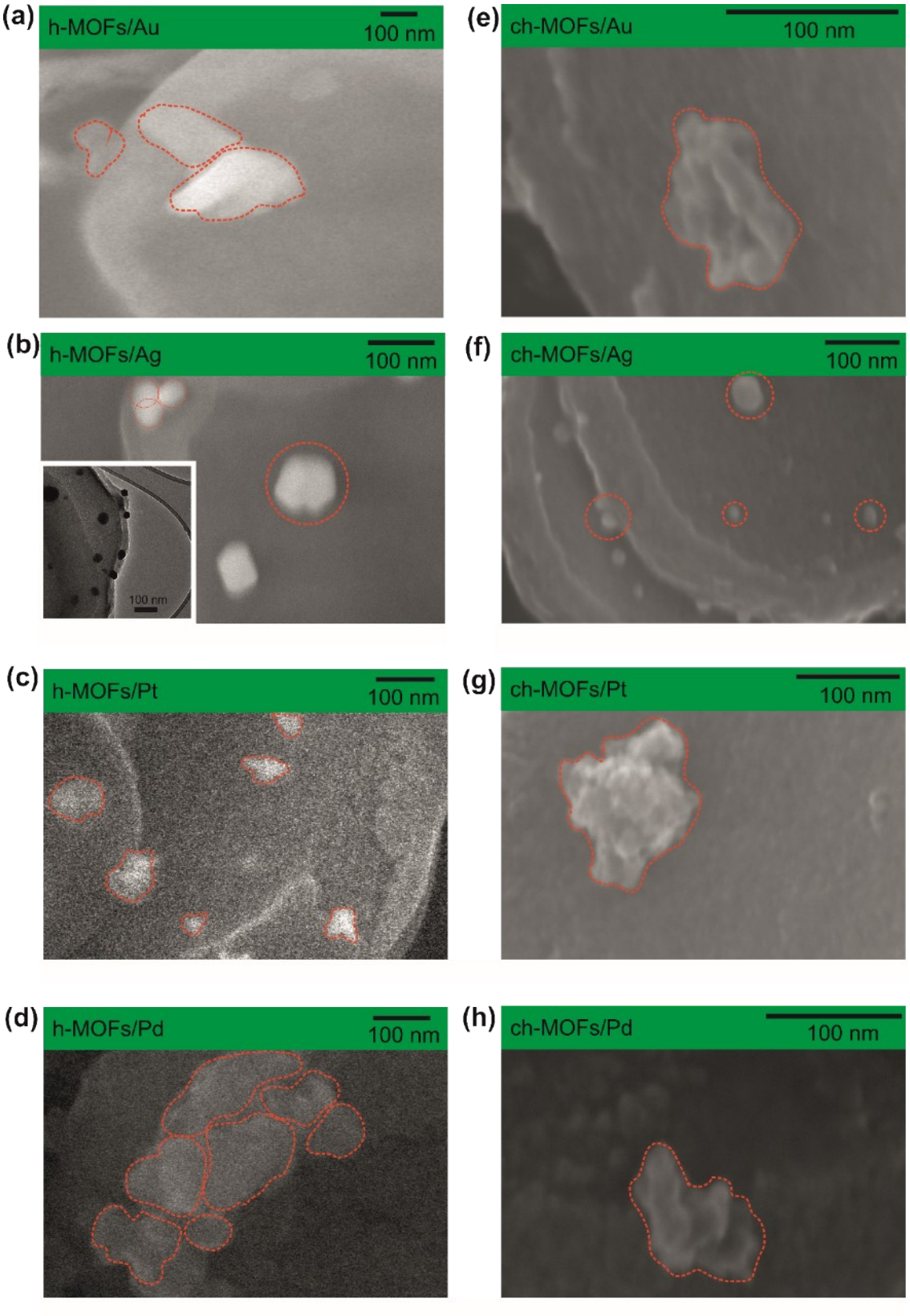

Fig. S2. SEM images of (a) h-MOFs/Au; (b) h-MOFs/Ag (with TEM image as inswert); (c) h-MOFs/Pt; (d) h-MOFs/Pd; (e) ch-MOFs/Au; (f) ch-MOFs/Ag; (g) ch-MOFs/Pt; (h) ch-MOFs/Pd

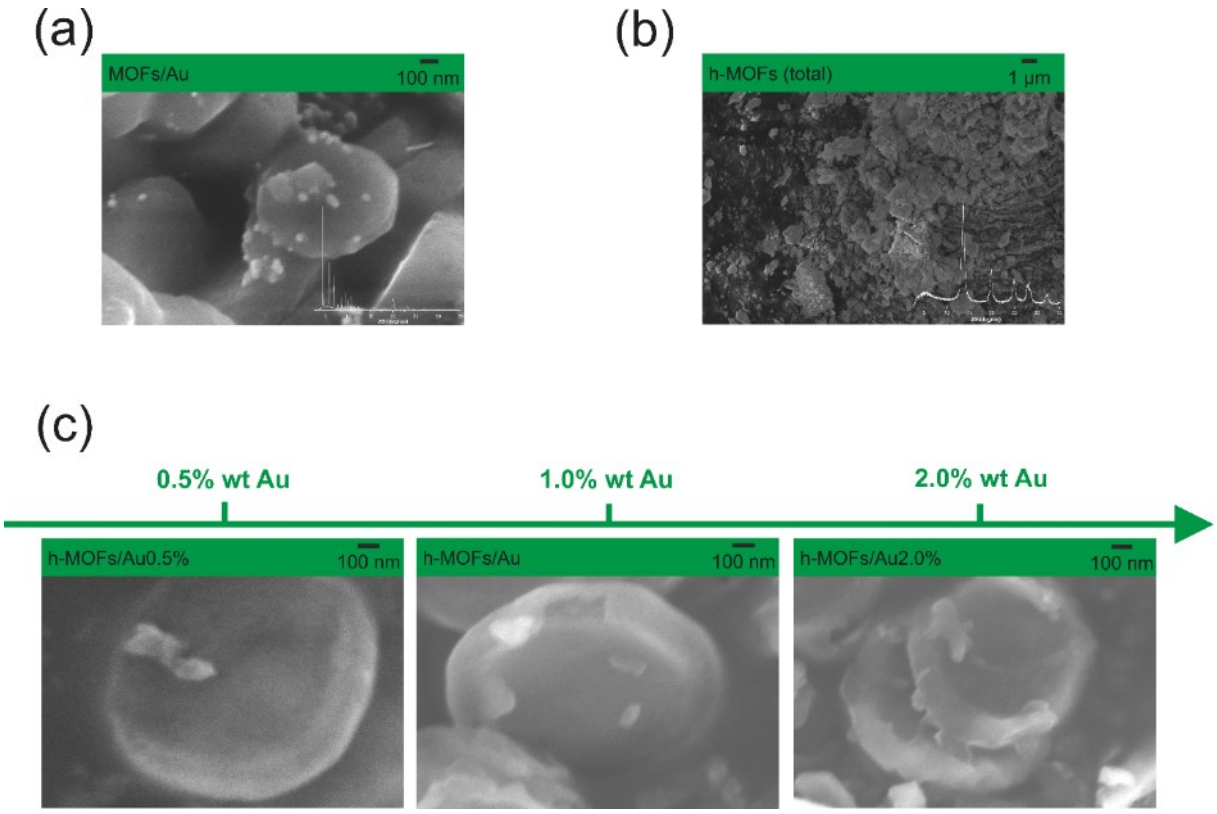

Fig. S3. SEM image of (a) MOFs/Au with XRD analysis as insert, (b) h-MOFs (total) with XRD analysis; and (c) h-MOF modifications with different amounts of Au (0.5, 1.0, and 2.0 wt%).

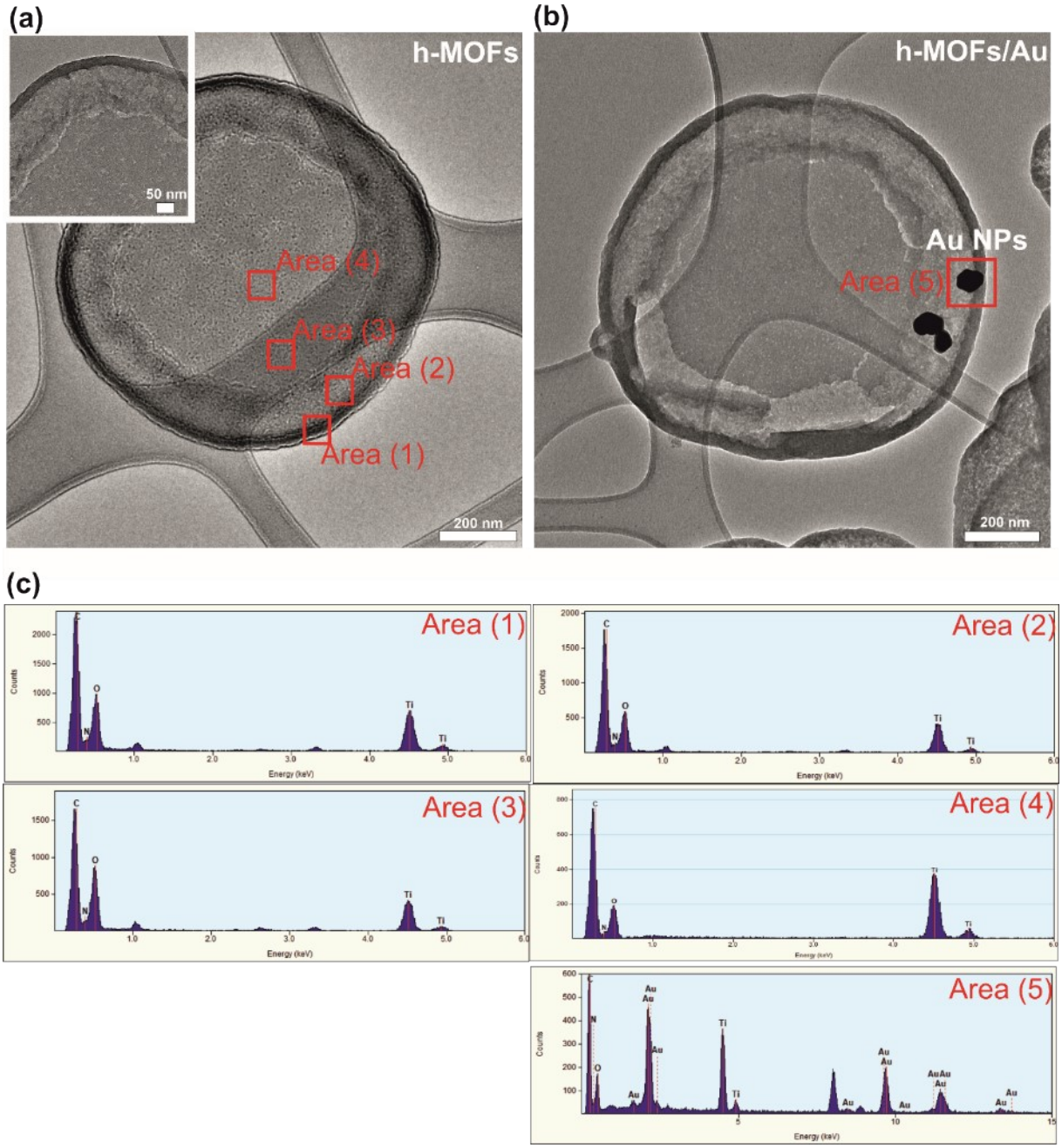

Fig. S4. TEM image of (a) h-MOFs and (b) h-MOFs/Au with (c) the corresponding EDS spectra.

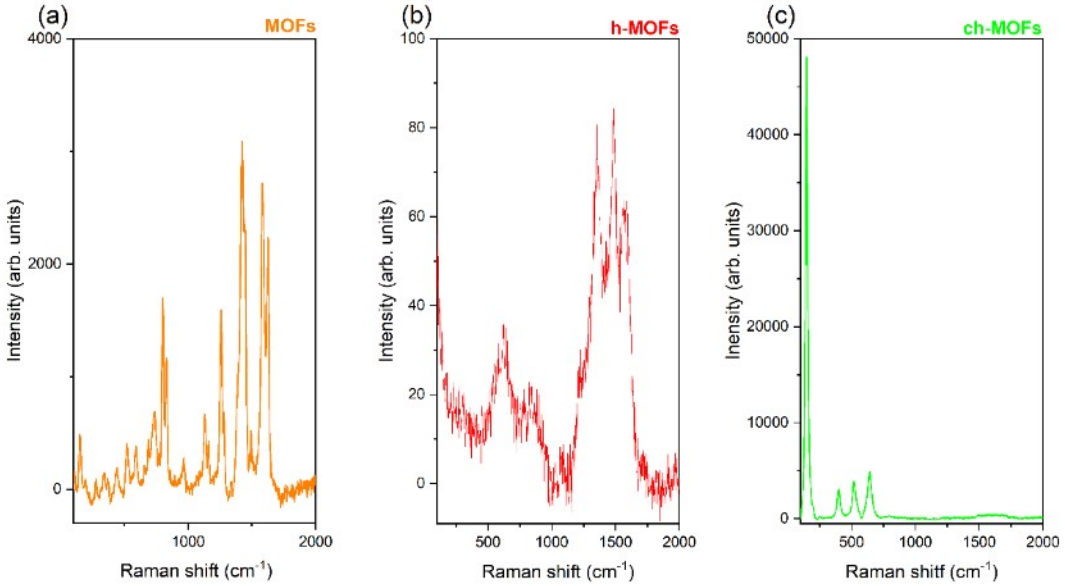

Fig. S5. Raman spectrum of MOF, h-MOF, and ch-MOF samples in the range of 100–2000 cm^{-}

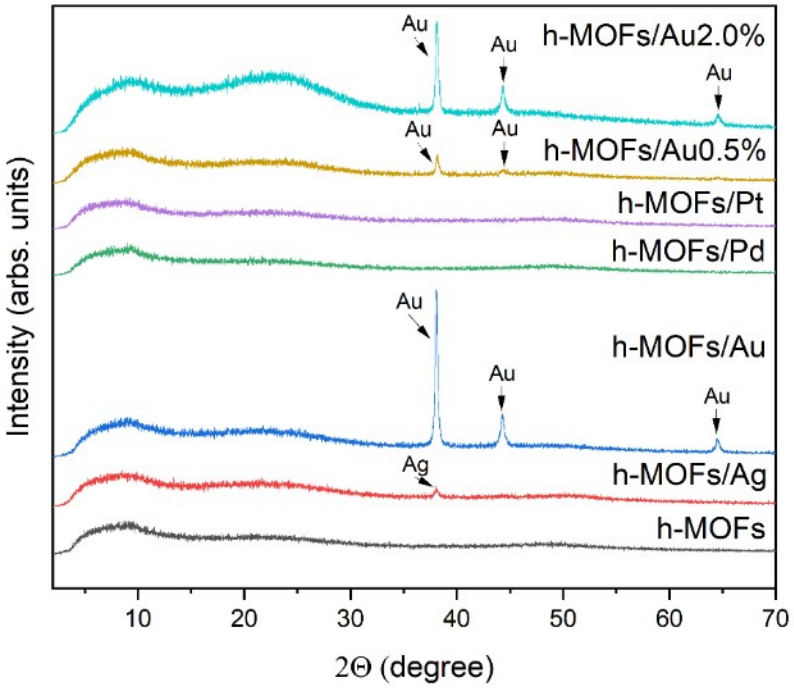

Fig. S6. XRD analysis for h-MOFs and modified samples in the range of 2–70° at 2Θ (degree).

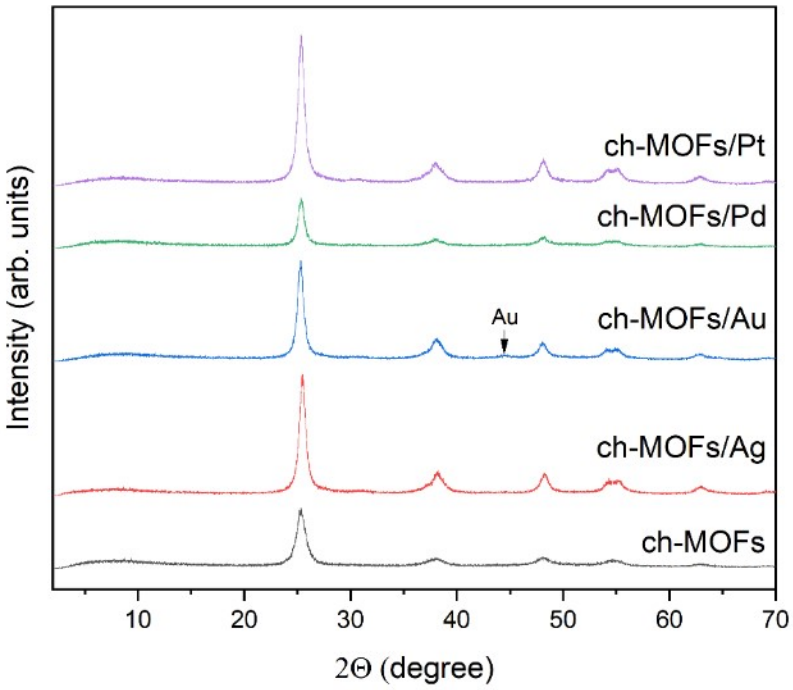

Fig. S7. XRD analysis for ch-MOFs and modified samples in the range of 2–70° at 2Θ (degree).

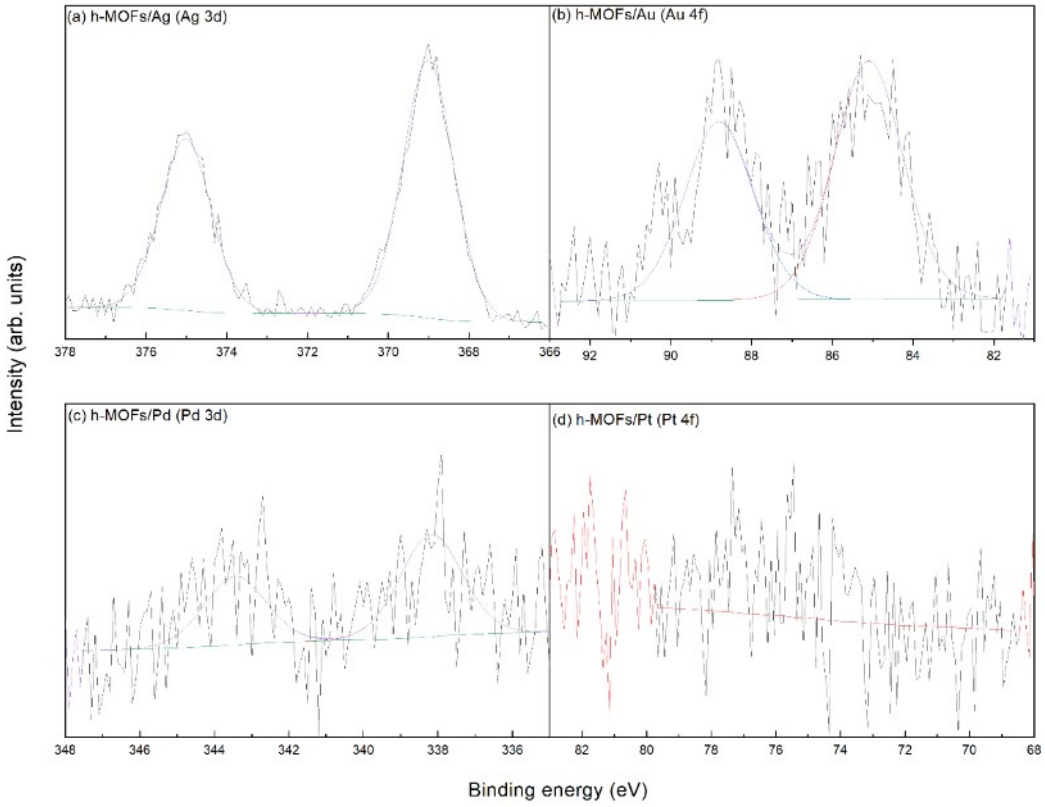

Fig. S8. High resolution spectra of the metals in the h-MOF/M samples: Ag 3d (a), Au 4f (b), P 3d (c), and Pt 4f (d).

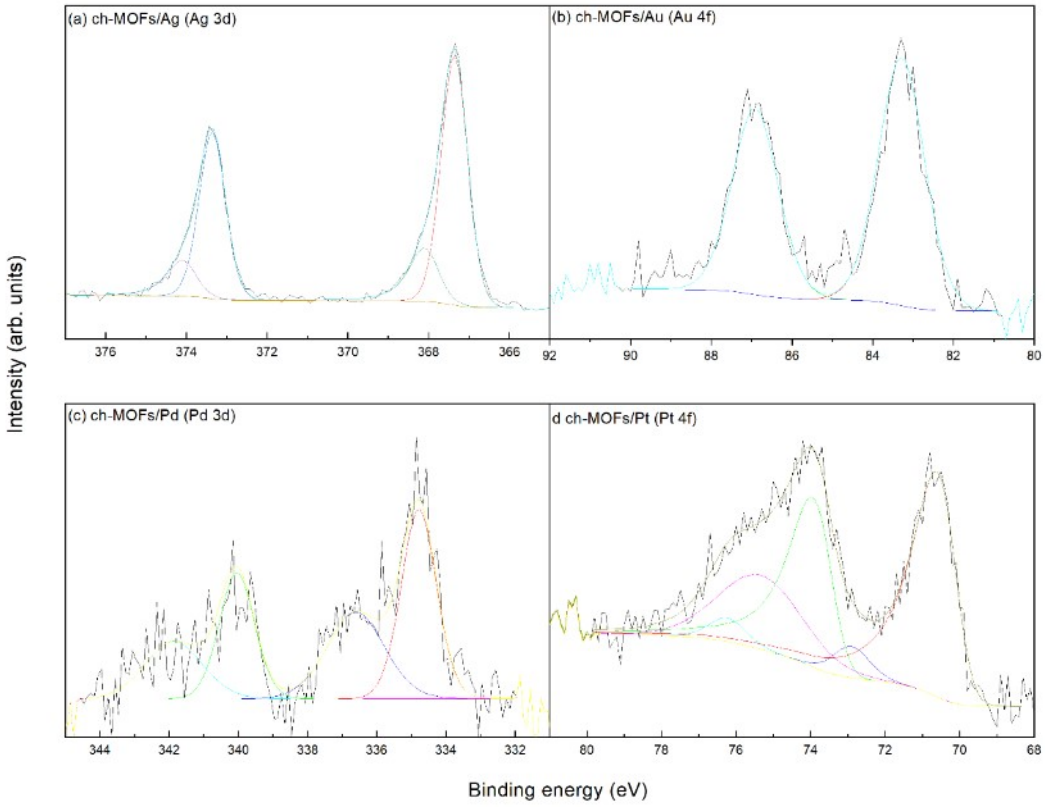

Fig. S9. High resolution spectra of the metals in the ch-MOF/M samples: Ag 3d (a), Au 4f (b), P 3d (c), and Pt 4f (d)

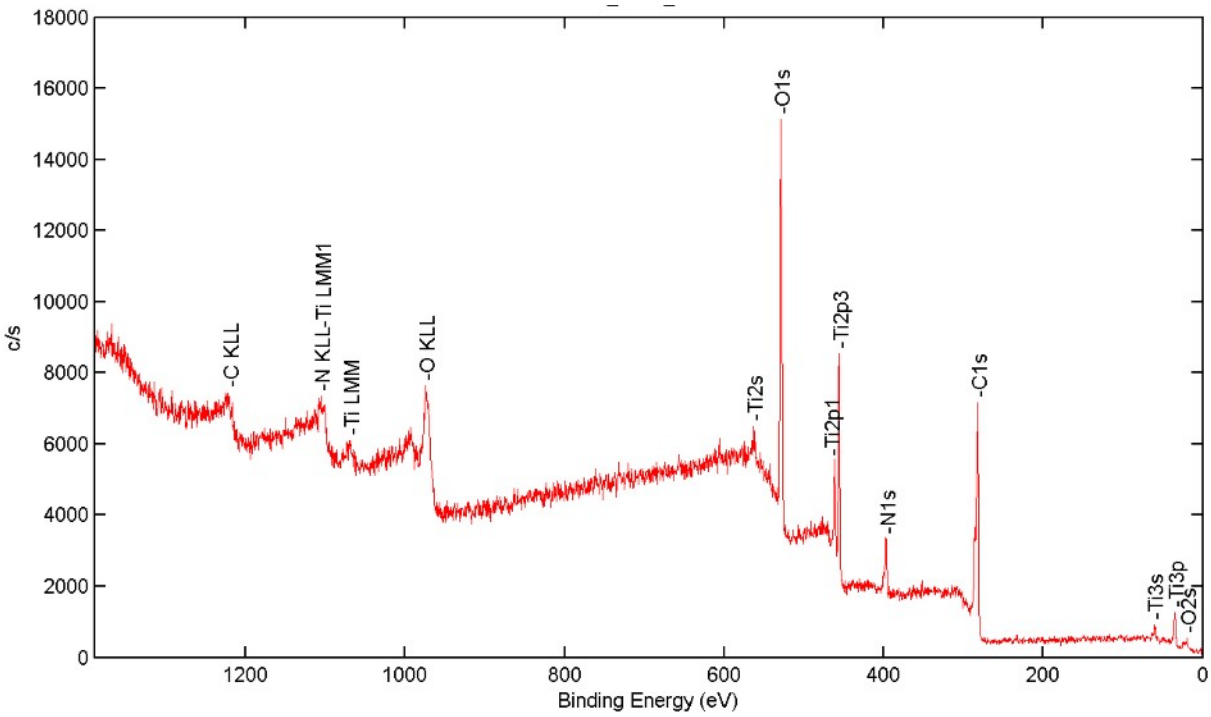

Fig. S10. XPS survey spectrum for a MOF sample.

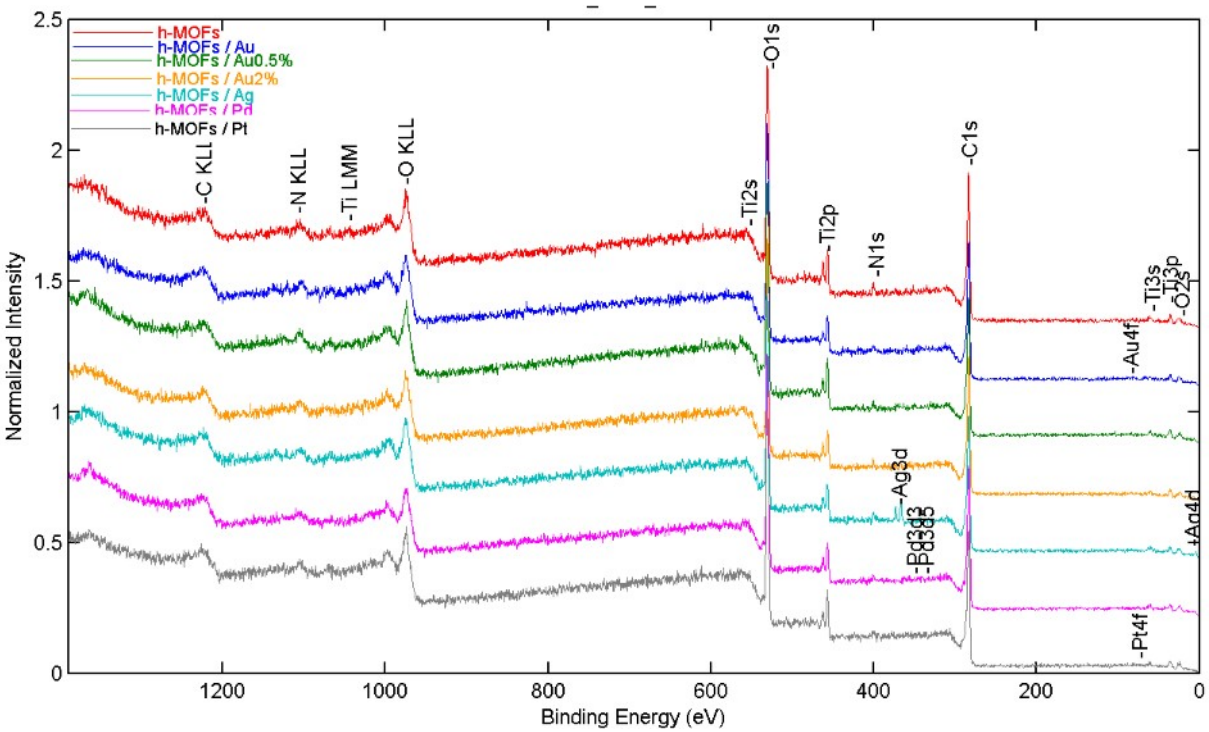

Fig. S11. XPS survey spectrum for h-MOF samples.

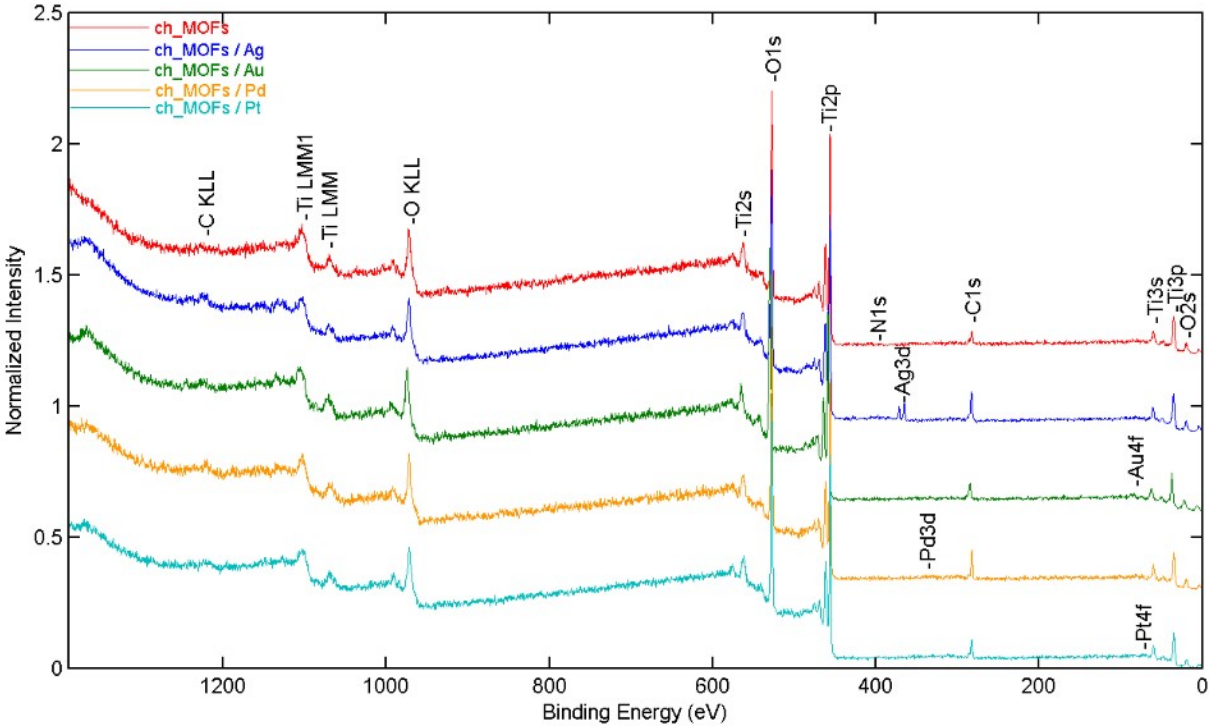

Fig. S12. XPS survey spectrum for ch-MOF samples.

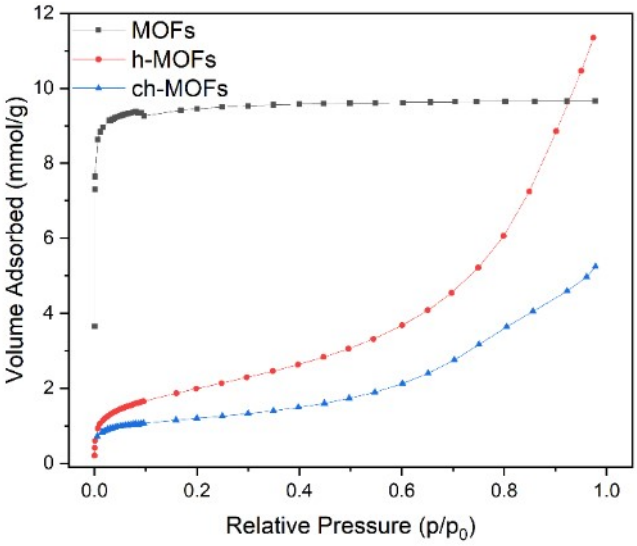

Fig. S13. Nitrogen adsorption BET isotherm of samples.

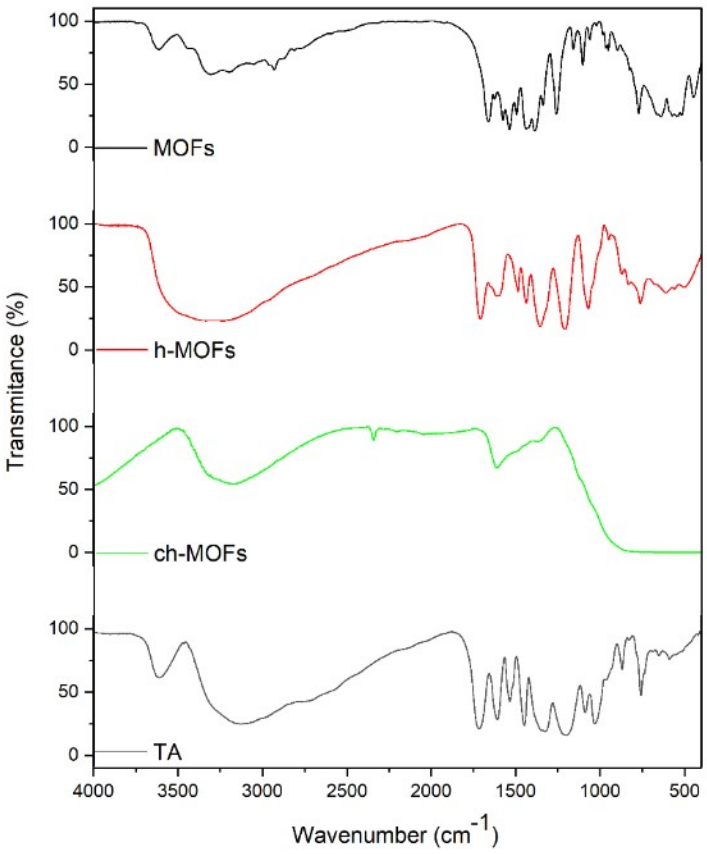

Fig. S14. FTIR spectra in the 400–4000 cm^{-1} range for the MOF samples and tannic acid (TA).

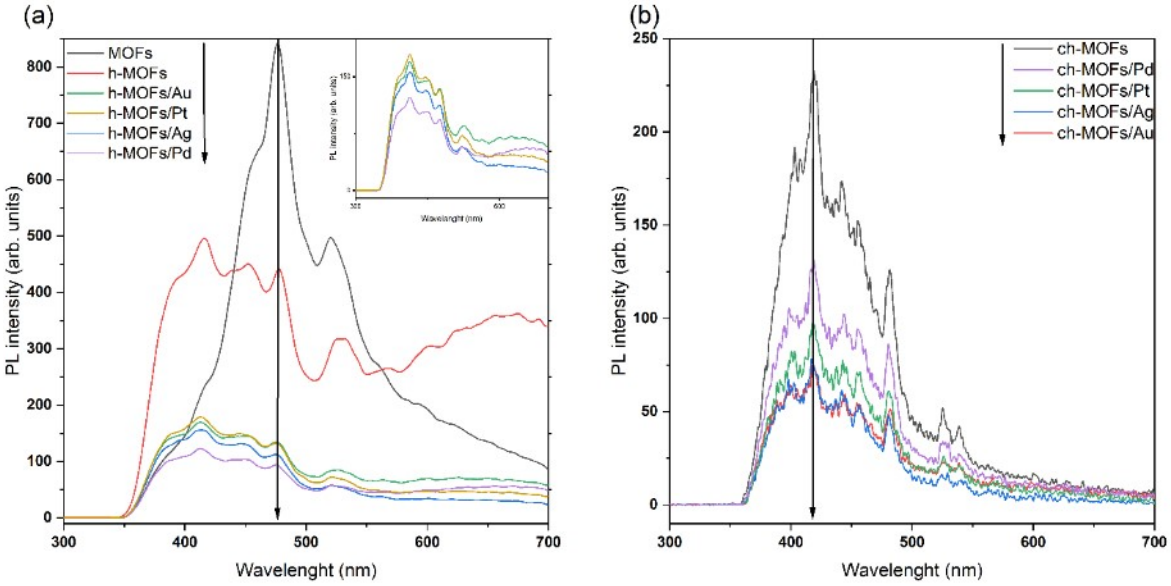

Fig. S15. PL spectra of (a) pristine MOFs and) hydrolyzed and (b) calcined composites of MOFs.

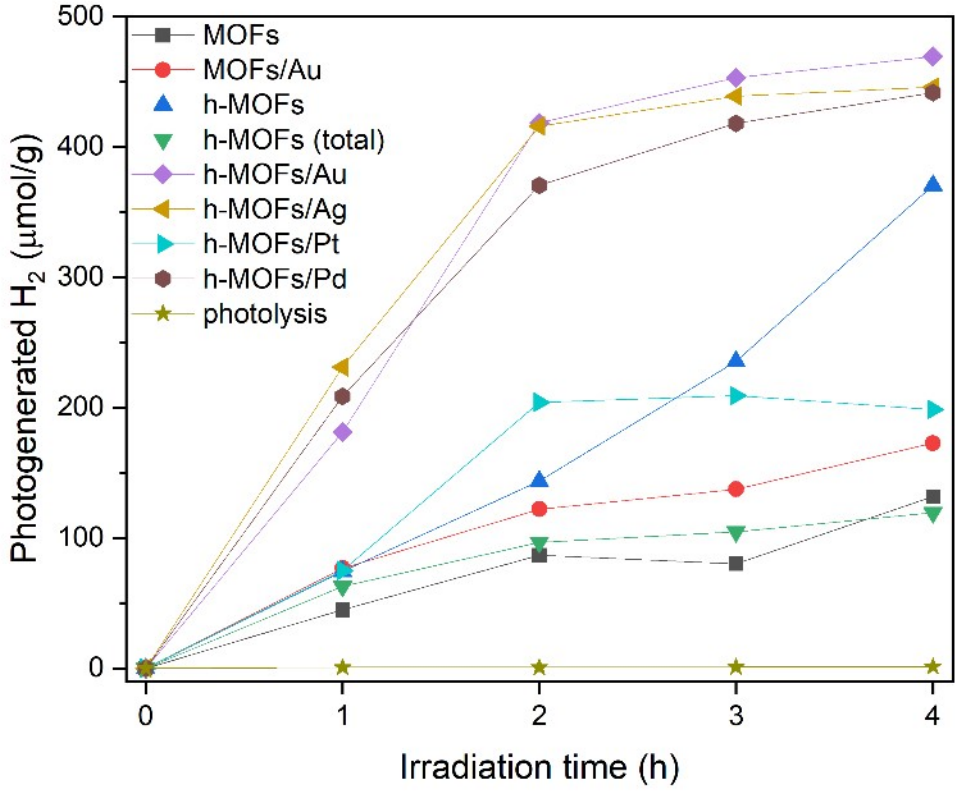

Fig. S16. Kinetics of hydrogen photogeneration in the presence of MOFs, h-MOFs, and corresponding noble metal–modified samples under UV-Vis irrigation.

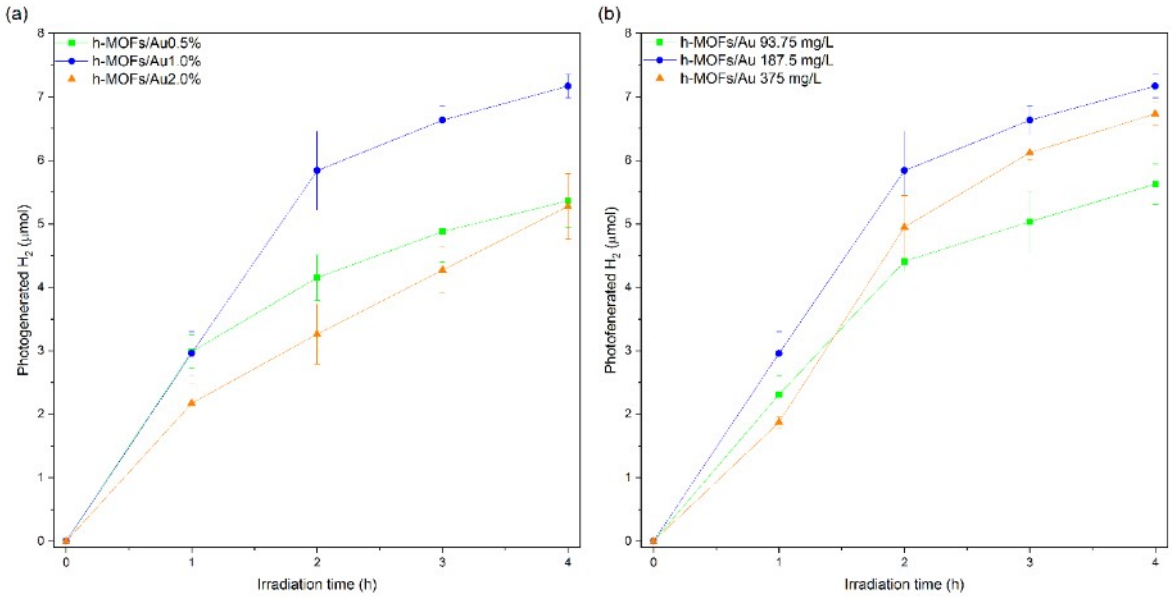

Fig. S17. Hydrogen evolution kinetics. (a) h-MOFs modified with different amounts of Au (% wt.) or (b) with different amounts of the h-MOFs/Au photocatalyst.

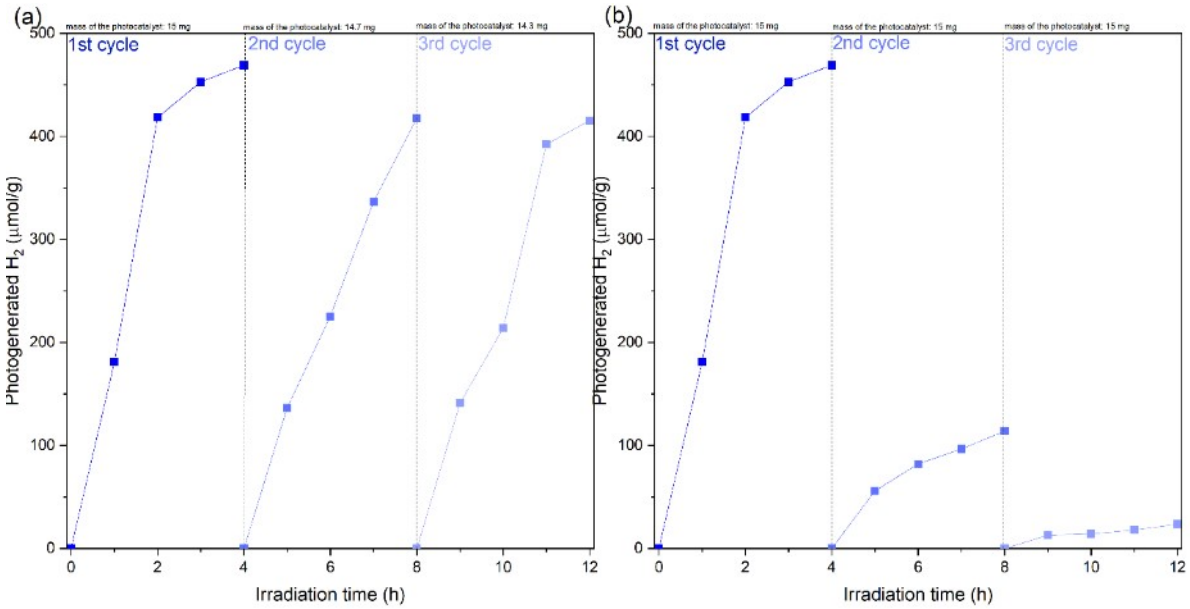

Fig. S18. Efficiency of hydrogen photogeneration in the presence of h-MOFs modified with Au under UV-Vis irradiation (a) over 3 cycles with electrolyte replacement, (b) over 3 cycles without electrolyte replacement.

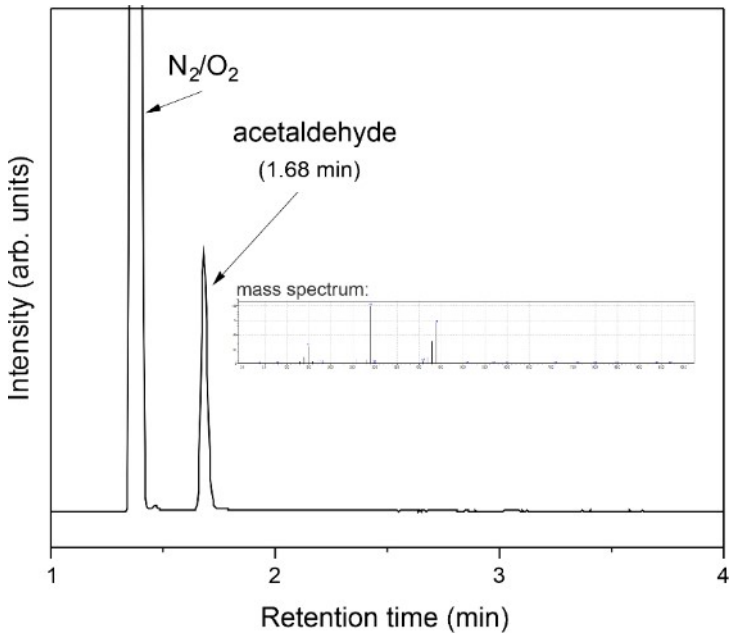

Fig. S19. Chromatograph produced by headspace-GC-MS analysis with signal from acetaldehyde highlighted (mass spectrum shown).

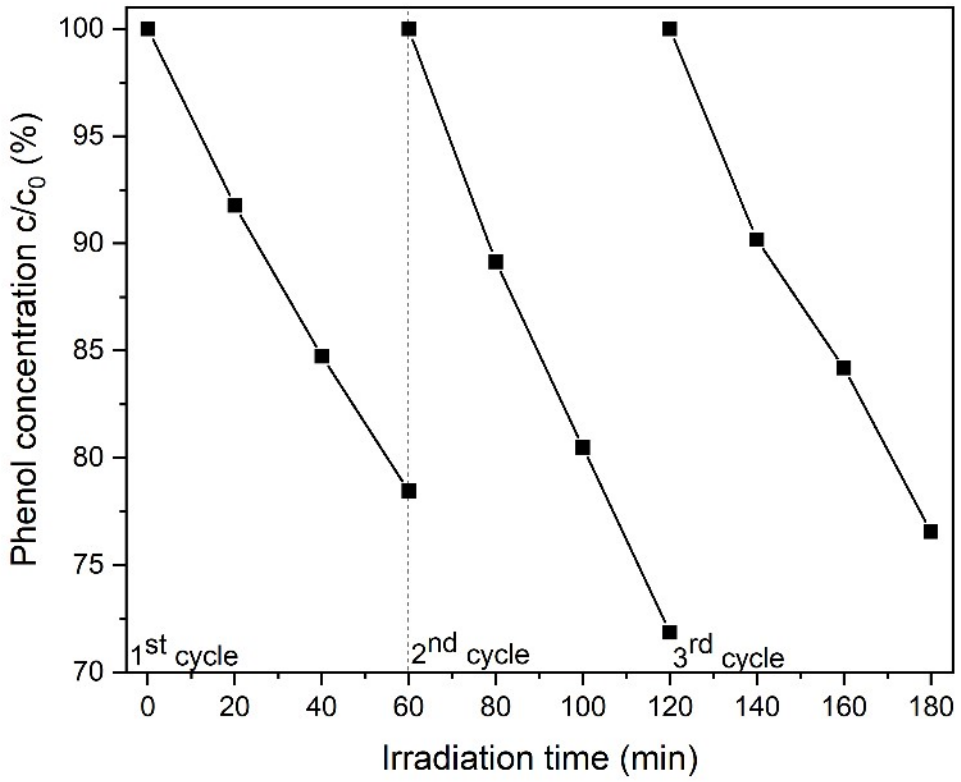

Fig. S20. Photostability of ch-MOFs/Au during three cycles of phenol photodegradation under Vis light.

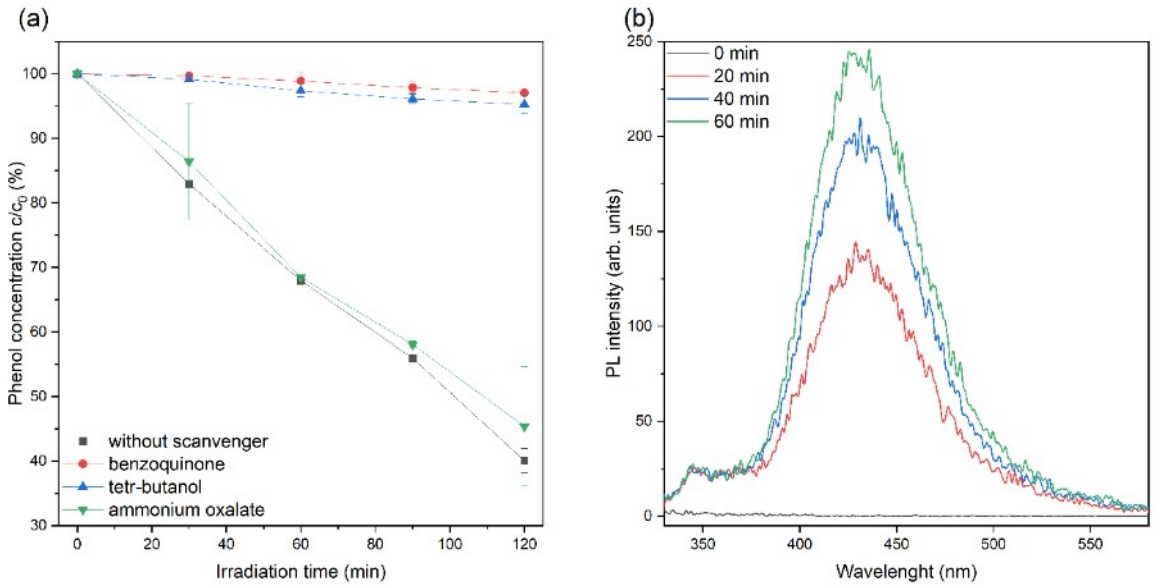

Fig. S21. (a) Photodegradation kinetics of phenol using ch-MOFs/Au in the presence of different scavengers under Vis light. (b) PL spectra changes of terephthalic acid solution over 60 min under Vis light irradiation using ch-MOFs/Au.